Journal of Computational Acoustics, Vol. 9, No. 2 (2001) 671–680

HIGHER-ORDER MASS-LUMPED FINITE ELEMENTS FOR THE WAVE EQUATION*

W. A. MULDER
Shell International Exploration and Production BV,
P.O. Box 60, NL-2280 AB Rijswijk, The Netherlands
E-mail: w.a.mulder@siep.shell.com

Received 20 July 1999
Revised 29 March 2000

The finite-element method (FEM) with mass lumping is an efficient scheme for modeling seismic wave propagation in the subsurface, especially in the presence of sharp velocity contrasts and rough topography. A number of numerical simulations for triangles are presented to illustrate the strength of the method. A comparison to the finite-difference method shows that the added complexity of the FEM is amply compensated by its superior accuracy, making the FEM the more efficient approach.

1. Introduction

The finite-difference method (FDM) is a popular numerical technique for the simulation of wave propagation through air, water, and solids. The method is relatively easy to implement and allows for straightforward parallelization. For realistic three-dimensional computations, storage is a bottleneck. For that reason, higher-order schemes are often chosen to keep numerical dispersion within acceptable limits while still using a moderate number of points per wavelength. However, this approach breaks down if sharp contrasts in material properties on regular cartesian grids need to be modeled. In the worst case with the most naive scheme, the numerical error becomes of first-order in the grid spacing, as a sampled velocity model does not distinguish variations on smaller length scales. Smoothing of material properties may help, as shown by for instance Muir *et al.*[1] Local modification of the finite-difference operator is another option; one of many examples is presented by Sochacki *et al.*[2] In general, these modification result in numerical errors of low-order, albeit better than first-order. The ultimate sharp contrast is the free surface. One approach to deal with rough topography is by assuming a vacuum or near-vacuum,[3] another is the use of a modified difference operator,[4] or a fictitious domain approach.[5] Again, these modifications generally lead to schemes of low-order.

Finite elements for triangles and tetrahedra are better suited to model rough topography and sharp interfaces between different materials, because these can be fitted by the element

*Presented at ICTCA'99, the 4th International Conference on Theoretical and Computational Acoustics, May 1999, Trieste, Italy.

boundaries. The finite-element method (FEM) in its original form requires the solution of a large sparse linear system of equations, which makes the method costly. This cost can be avoided by mass lumping, a technique that replaces the large linear system by a diagonal matrix.[6] To avoid negative integration weights that cannot produce a stable time-stepping scheme, additional nodes have to be added to the element. Initial results for triangular elements are due to Tordjman *et al.*[7–9] The extension of this idea to triangular elements of still higher order and to tetrahedra can be found in a report by Mulder.[10] There, it was also shown by a comparison on a simple two-dimensional reflection problem that the higher-order FEM can be more efficient than the FDM. A comparison between finite-element schemes of various orders revealed that the higher-order approximations are more efficient than the lower-order elements. This motivated the search for elements of still higher-order.[11]

Here, the finite-element scheme and some implementation details are described in Sec. 2. In Sec. 3, two 2-D examples are given of the method, one in a marine environment with a salt dome, and one for a hilly area. For the former, a comparison to the finite-difference method is included.

2. Finite Elements

2.1. *Construction of elements*

Let the wave equation for constant-density acoustics be given by

$$\frac{1}{c(x)^2}\frac{\partial^2}{\partial t^2}u(t,x) = \Delta u(t,x) + f(t,x)\,, \tag{2.1}$$

on a domain $\Omega \subset \mathbb{R}^{n_{\rm dim}}, n_{\rm dim} = 2$ or $n_{\rm dim} = 3$, with source term $f(t,x)$, $x \in \Omega$ and $t \in (0,T) \subset \mathbb{R}$. Initial values $u(0,x)$ and $\frac{\partial}{\partial t}u(0,x)$ are assumed to be zero; here only zero Dirichlet boundary conditions are considered. The weak formulation for this problem is

$$\int_\Omega dx \left[c^{-2}\frac{\partial^2 u}{\partial t^2}v + \nabla_x u \cdot \nabla_x v - fv\right] = 0\,, \tag{2.2}$$

for all test functions $v \in H_0^1(\Omega)$.

The finite-element discretization is obtained in the usual way. Given a grid made up of N_t triangles or tetrahedra $\mathcal{T}_j, j = 1,\ldots,N_t$, a set of n_t nodes is defined for each element. On each element, shape functions are defined as polynomials that equal 1 on one of the nodes and 0 on the other nodes. The polynomials are chosen in such a way that mass lumping can be applied without loss of accuracy. This means that polynomials up to a degree $q = 2M-2$ should be integrated exactly by numerical quadrature, if shape functions of a maximum degree M are considered. This, however, generally leads to zero of negative integration weights, as shown by Tordjman *et al.*[7–9] Stricly positive weights are needed for stability. Such weights can be found if a larger space of polynomials is considered. For triangles, polynomials of maximum degree M_f that have a restriction to the edges of at most a degree $M \le M_f$ can be used. The integration rule should then be exact for polynomials up

to degree $q = M + M_f - 2$. In this enlarged space, a known element[12] of third-order ($M = 2$) and a new element of fourth-order ($M = 3$) were found.[7–9] In a paper by Mulder,[10] the extension to tetrahedra was accomplished by using polynomials of highest degree M_i in the interior, with a restriction to the faces of highest degree $M_f \leq M_i$ and a restriction to the edges of highest degree $M \leq M_f$. A third-order element was found ($M = 2$, $M_f = M_i = 4$). Also, a new element for triangles of fifth-order ($M = 4$, $M_f = 5$) was discovered and reported in the same paper. A systematic search[11] based on the theory of consistency conditions for numerical quadrature[13–15] resulted in a new sixth-order element ($M = 5$, $M_f = 7$) for triangles and a new fourth-order element for tetrahedra ($M = 3$, $M_f = 5$, $M_i = 6$).

To construct these higher-order elements, the following steps need to be carried out. First, a set of polynomials and supporting nodes have to be chosen. The nodes are chosen in a symmetric arrangement, and the polynomials are required to be continuous from one element to the next. This implies that the vertices are included and that there must be sufficient nodes on the edges (and faces in 3-D) to uniquely define the restriction of the polynomials to the edges (and faces). Secondly, moment equations are formed stating that the numerical integration of these polynomials must be exact up to a certain degree. Thirdly, the nonlinear system of moment equations need to be solved. The system of moment equations is linear in the integration weights and polynomial in the parameters that define the position of (some of) the nodes. If one or more solutions exist, the ones with strictly positive weights needs to be selected, because zero or negative integration weights lead to an unstable time-stepping scheme. The theory of consistency conditions provides those choices for the polynomials and associated nodes, that are likely to produce a nonlinear system of equations that has at least one solution. The solution of this nonlinear system is currently a bottleneck for the construction of elements of still higher-order, even when Gröbner basis techniques[16] are used.

A summary of elements for triangles is listed in Table 1, from second to sixth-order ($M = 1, \ldots, 5$). For each element, the maximum degree of polynomials on the edges (M) and in the interior (M_f) is given, followed by a list of nodes. For each node, only one point of the equivalence class is given; the other nodes follow by symmetry. The number of nodes in the equivalence class is given next, followed by the corresponding integration weight for numerical quadrature. In the last column, the parameters defining the position of the node are given, namely α, β, and so on. The positions of the nodes have been drawn in Fig. 1 for a triangle with normalized coordinates. Results for tetrahedra can be found elsewhere.[11]

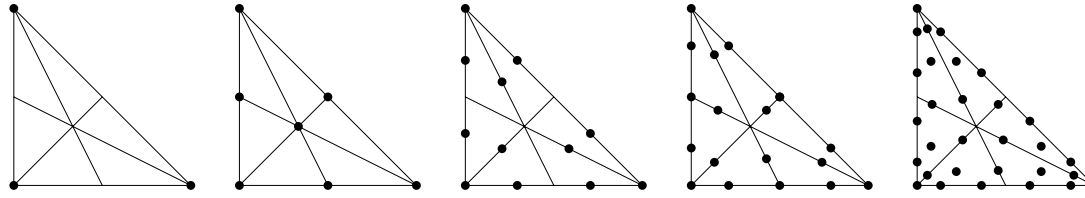

Fig. 1. Nodes for elements of second ($M = 1$) to sixth-order ($M = 5$), from left to right.

Table 1. Triangular elements.

M	M_f	Nodes	Number	Weights	Position Parameters
1	1	$(0,0)$	3	$\frac{1}{6}$	–
2	3	$(0,0)$	3	$\frac{1}{40}$	–
		$\left(\frac{1}{2},0\right)$	3	$\frac{1}{15}$	–
		$\left(\frac{1}{3},\frac{1}{3}\right)$	1	$\frac{9}{40}$	–
3	4	$(0,0)$	3	$\frac{1}{90}-\frac{\sqrt{7}}{720}$	–
		$(\alpha,0)$	6	$\frac{7}{720}+\frac{\sqrt{7}}{180}$	$\frac{1}{2}-\frac{\sqrt{441-84(7-\sqrt{7})}}{42}$
		(β,β)	3	$\frac{49}{360}-\frac{7\sqrt{7}}{720}$	$\frac{1}{3}(1-\frac{1}{\sqrt{7}})$
4	5	$(0,0)$	3	$\frac{1}{315}$	–
		$\left(\frac{1}{2},0\right)$	3	$\frac{4}{315}$	–
		$(\alpha,0)$	6	$\frac{3}{280}$	$\frac{1}{2}(1-\frac{1}{\sqrt{3}})$
		(β_1,β_1)	3	$\frac{163}{2520}+\frac{47\sqrt{7}}{8820}$	$\frac{5+\sqrt{7}}{18}$
		(β_2,β_2)	3	$\frac{163}{2520}-\frac{47\sqrt{7}}{8820}$	$\frac{5-\sqrt{7}}{18}$
5	7	$(0,0)$	3	0.709423970679245OE-03	–
		$(\alpha_1,0)$	6	0.619056500367662 9E-02	0.363298074153686 0E-00
		$(\alpha_2,0)$	6	0.348057864048921 1E-02	0.132264581632714 0E-00
		(β_1,β_1)	3	0.345304303772827 9E-01	0.457836838079161 1E-00
		(β_2,β_2)	3	0.459012376307628 6E-01	0.256859107261959 1E-00
		(β_3,β_3)	3	0.116261354596175 7E-01	0.575276844114101 1E-01
		(γ_1,δ_1)	6	0.272785759699962 6E-01	0.781925836255170 2E-01
					0.221001218759890 0E-00

2.2. *Implementation details*

The semi-discrete finite-element discretization of Eq. (2.2) is given by

$$\mathcal{M}^h \frac{\partial^2 u^h(t)}{\partial t^2} + \mathcal{K}^h u^h(t) = F^h\,, \tag{2.3}$$

where F^h is the discrete source term, $\mathcal{M}^h$ the mass matrix, which is replaced by a diagonal matrix $\tilde{\mathcal{M}}^h$ using mass lumping, and $\mathcal{K}^h$ the stiffness matrix. The latter is evaluated analytically as follows. The contribution per element is expressed in normalized coordinates.

In these coordinates, we have a sum of three matrices of size $n_t \times n_t$, multiplied by scalar factors that account for the local coordinate transformation. Recall that n_t is the number of nodes per element. The three matrices can be evaluated once, using a symbolic manipulation package such as, for instance, *Mathematica*.

A second-order time-stepping scheme is

$$u^h(t^{n+1}) = 2u^h(t^n) - u^h(t^{n-1}) + (\Delta t)^2[L^h u^h(t^n) + F^h(t^n)]\,, \quad L^h = (\tilde{\mathcal{M}}^h)^{-1}\mathcal{K}^h\,. \tag{2.4}$$

Here, $t^n = t^0 + n\Delta t$. Higher-order time stepping is obtained with the scheme by Dablain,[17] which requires repeated application of the spatial operator (once for every two temporal orders of accuracy).

Absorbing boundaries are implemented by enlarging the computational domain and applying a simple damping term.[18] This changes Eq. (2.4) into

$$u^h(t^{n+1}) = u^h(t^n) + (1-\gamma)[u^h(t^n) - u^h(t^{n-1})] + (\Delta t)^2[L^h u^h(t^n) + F^h(t^n)]\,. \tag{2.5}$$

Here γ is chosen as a function of distance to the boundary. Let r denote the distance to the boundary of the original problem, then $\gamma = \varepsilon_b \Delta t (r/r_{\max})^2$, where $\varepsilon_b \Delta t$ should be much smaller than one, typically a few percent, and $r_{\max}$ is the width of the strip added to the domain of the original problem.

Note that the introduction of γ somewhat reduces the maximum time-step allowed for stability. More precisely, let ρ be the spectral radius of the non-negative operator $R = -(\Delta t)^2 L^h$. For Dablain's scheme with an even temporal order of accuracy N_t, the stability condition is

$$\sum_{m=1}^{N_t/2} \frac{2}{(2m)!}\rho^m \le 4 - 2\gamma\,. \tag{2.6}$$

The spectral radius of R may be estimated by taking the maximum row sum of absolute values of its elements.

The pressure field at arbitrary receiver positions is computed by polynomial interpolation using the same polynomials as for the discretization.

3. Examples

An example of seismic wave propagation around a salt diapir is shown in Figs. 2–4. The domain size is 6 by 3 km, and velocities range from 1500 m/s in the water layer at the top to 5500 m/s in the salt. The finite-element grid is shown in Fig. 2. The area of the triangles is roughly proportional to the square of the velocity. A shot is fired in the water layer at a depth of 10 m and an offset of 2 km from the left of the figure. The position of the source has been marked by a dot in Fig. 2. The signal is recorded by 121 receivers to the right of the source starting at 2100 m offset, with 25 m horizontal spacing, and at 10 m depth. The order of the FEM scheme is 5 in space and 4 in time.

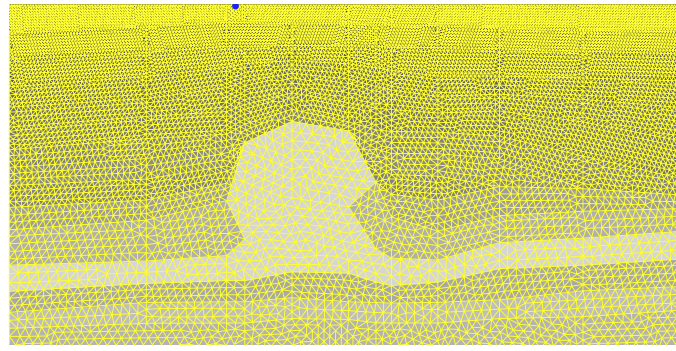

Fig. 2. Finite-element grid for a salt diapir problem.

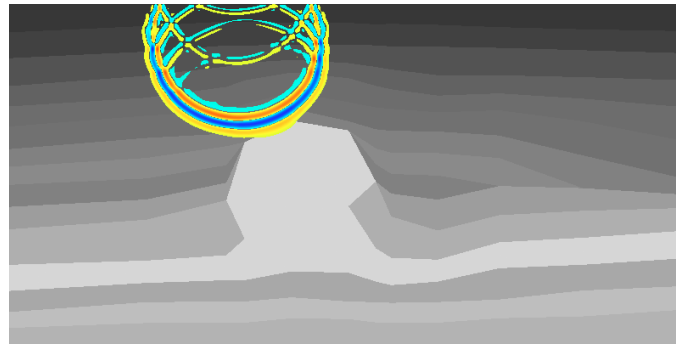

Fig. 3. Wave fronts after 0.5 seconds.

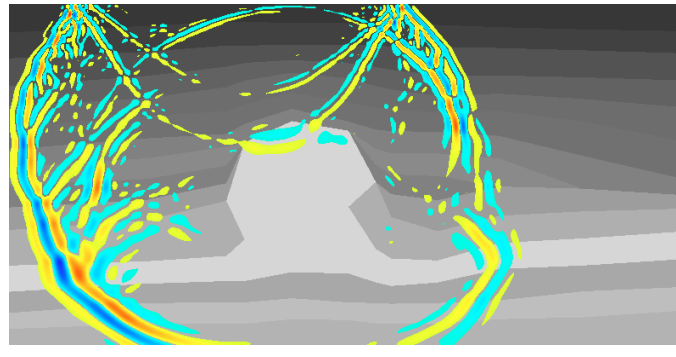

Fig. 4. Wave fronts after 1.0 seconds.

Figures 3 and 4 show snapshots of the wavefronts at 0.5 and 1.0 seconds. The recorded receiver data are shown in Fig. 5.

To get an impression of the FEM method in comparison to the FDM, traces were computed by a FDM scheme of order 4 in both space in time. The relative error of the FDM method was estimated by computing traces for a grid with 10 m spacing in both x and

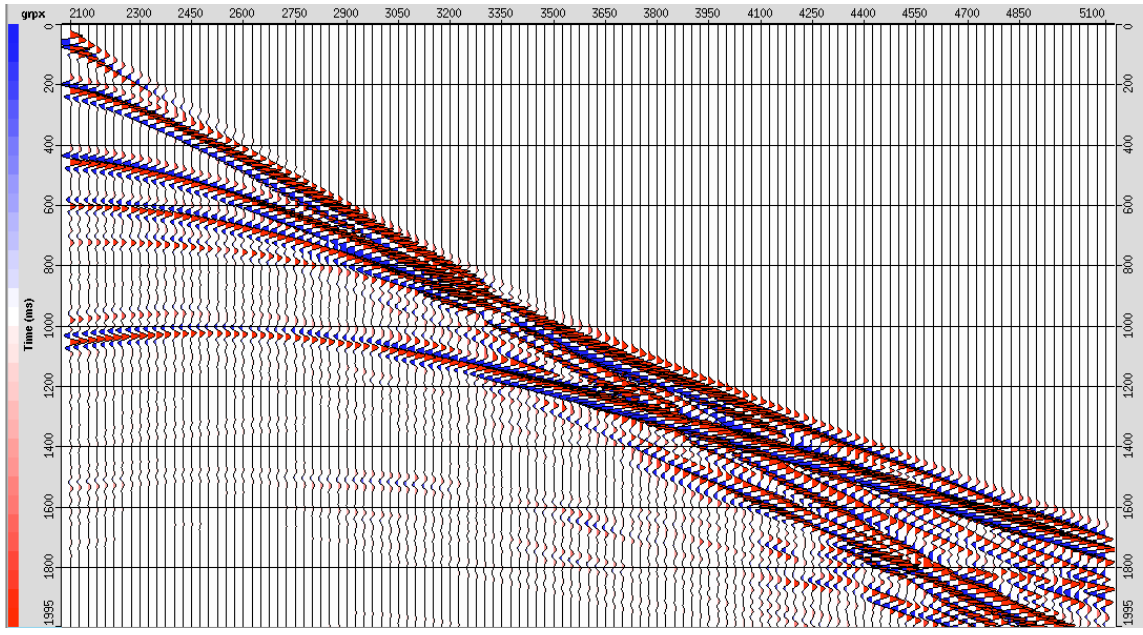

Fig. 5. Receiver traces.

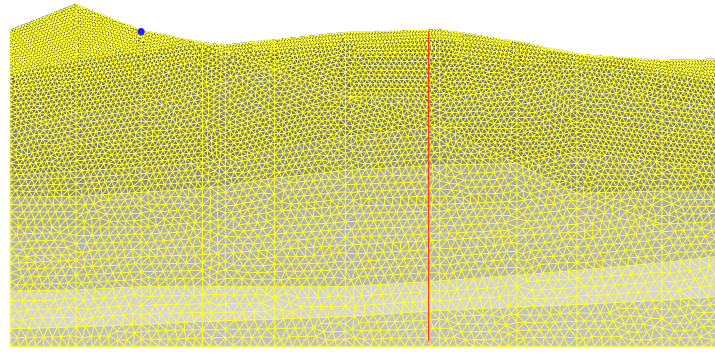

Fig. 6. Finite-element grid for a problem in a hilly region.

z and a time-step of 0.25 ms and 801×401 unknowns, and with 5 m spacing, 0.125 ms time-step, and 1601×801 unknowns, which took 8 times longer to compute. The same was done for the FEM method, with a grid of 7439 triangles and 82460 unknowns and a grid of 29244 triangles (Fig. 2) with 322909 unknowns, using order 5 in space and 4 time. Note that the number of degrees of freedom for the FEM was chosen considerably smaller than for the FDM to get almost the same amount of cpu time. The reason is that the FDM has a smaller operation count per unknown than the FEM. The result of this comparison is a relative error for the FEM that is about 35% smaller as for the FDM. Here the relative error was measured by taking the root-mean-square norm of the differences between the traces

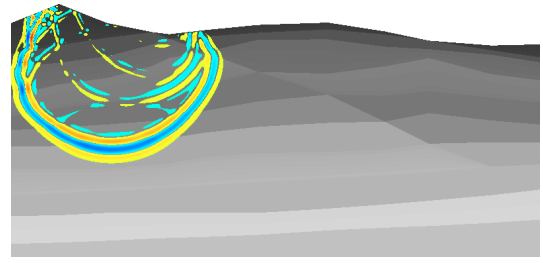

Fig. 7. Snapshot at 0.5 seconds.

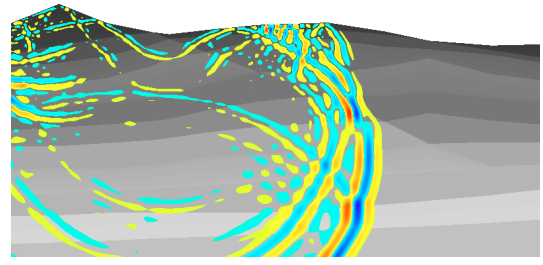

Fig. 8. Snapshot at 1.0 seconds.

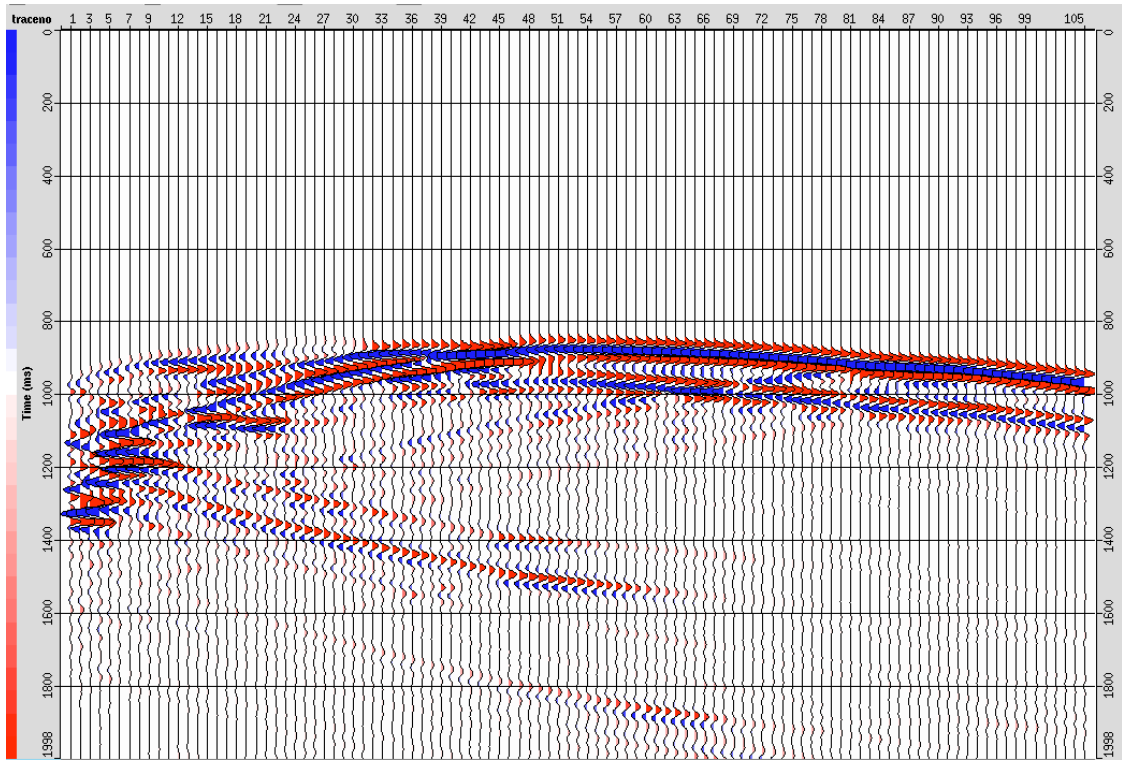

Fig. 9. Receiver traces.

obtained on the coarser and the finer grid. The result suggests that the FEM is more efficient than the FDM for this specific example.

The next example is a Vertical Seismic Profiling (VSP) shot in a hilly region. The receivers are located in a well. The lateral size of the domain is 6 km, the depth 2.86 km measured from the highest surface point. The velocities range from 1700 m/s to 5590 m/s. The grid is shown in Fig. 6. The receiver positions are indicated in Fig. 6 by the vertical line, starting at a depth of 10 m below the surface and having a depth spacing of 25 m. Also shown is the position of the source, marked by a dot. Figures 7 and 8 show snapshots of the wavefronts at intervals 0.5 and 1.0 seconds. The recorded traces in are presented in Fig. 9.

4. Conclusions

Higher-order finite elements are well-suited for modeling wave propagation in media with abrupt changes in material properties and with irregular surfaces. With mass lumping, the complexity of the finite-element method is the same as a finite-difference or finite-volume method. Moreover, the superior accuracy in comparison to higher-order finite differences allows for the use of less degrees of freedom. In this way, the finite-element method can compete with or even outperform the finite-difference method on some problems. Here, the strength of the method has been illustrated by some two-dimensional examples.

The efficiency of the method in three dimensions with tetrahedral elements remains an open question. The higher-order mass-lumped tetrahedral elements have a large number of nodes compared to the standard higher-order elements without lumping. It may well be that the use of fast iterative solvers results in a scheme that is faster than the one with mass-lumped elements.

References

1. F. Muir, J. Dellinger, J. Etgen, and D. Nichols, "Modeling elastic fields across regular boundaries," *Geophysics* **57**, 1189 (1992).
2. J. S. Sochacki, J. H. George, R. E. Ewing, and S. B. Smithson, "Interface conditions for acoustic and elastic wave propagation," *Geophysics* **56**, 168 (1991).
3. D. M. Boore, "Finite difference methods for seismic wave propagation in heterogeneous materials," in *Methods in Computational Physics* **11**, ed. B. A. Bolt (Academic Press, New York, 1972), pp. 1–38 .
4. G. H. Shortley and R. Weller, "Numerical solution of Laplace's equation," *J. Appl. Phys.* **9**, 334 (1938).
5. F. Millot, F. Collino, and P. Joly, "Fictitious domain method for unsteady problems: Application to electromagnetic scattering," in *Proc. 3rd Int. Conf. on Mathematical and Numerical Aspects of Wave Propagation*, eds. G. Cohen, E. Bécache, P. Joly, and J. E. Roberts (SIAM, Philadelphia, 1995), pp. 260–269.
6. I. Fried and D. S. Malkus, "Finite element mass matrix lumping by numerical integration without convergence rate loss," *International Journal of Solids and Structures* **11**, 461 (1976).
7. G. Cohen, P. Joly, and N. Tordjman, "Construction and analysis of higher order finite elements with mass lumping for the wave equation," in *Proc. 2nd Int. Conf. on Mathematical and*

Numerical Aspects of Wave Propagation, eds. R. Kleinman, T. Angell, D. Colton, F. Santosa, and I. Stakgold (SIAM, Philadelphia, 1993), pp. 152–160.
8. G. Cohen, P. Joly, and N. Tordjman, "Higher order triangular finite elements with mass lumping for the wave equation," in *Proc. 3rd Int. Conf. on Mathematical and Numerical Aspects of Wave Propagation*, eds. G. Cohen, E. Bécache, P. Joly, and J. E. Roberts (SIAM, Philadelphia, 1995), pp. 270–279.
9. N. Tordjman, "Élements finis d'order élevé avec condensation de masse pour l'equation des ondes," Ph.D. thesis, L'Université Paris IX Dauphine, 1995.
10. W. A. Mulder, "A comparison between higher-order finite elements and finite differences for solving the wave equation," in *Proc. 2nd ECCOMAS Conf. on Numerical Methods in Engineering*, eds. J.-A. Désidéri, P. Le Tallec, E. Oñate, J. Périaux, and E. Stein (John Wiley & Sons, Paris, 1996), pp. 344–350.
11. M. J. S. Chin-Joe-Kong, W. A. Mulder, and M. van Veldhuizen, "Higher-order triangular and tetrahedral finite elements with mass lumping for solving the wave equation," *J. of Engineering Mathematics* (1999), pp. 405–426.
12. J. E. Akin, *Finite Element Analysis for Undergraduates* (Academic Press, London, 1986).
13. P. Keast and J. C. Diaz, "Fully symmetric integration formulas for the surface of the sphere in s dimensions," *SIAM J. Numerical Analysis* **20**, 406 (1983).
14. P. Keast, "Moderate-degree tetrahedral quadrature formulas," *Computer Methods in Applied Mechanics and Engineering* **55**, 339 (1986).
15. P. Keast, "Cubature formulas for the surface of the sphere," *J. of Computational and Applied Mathematics* **17**, 151 (1987).
16. B. Buchberger, "A criterion for detecting unnecessary reductions in the construction of Gröbner Bases," in *Lecture Notes in Computer Science,* Vol. 72 (Springer-Verlag, 1979), pp. 3–21.
17. M. A. Dablain, "The application of higher-order differencing to the scalar wave equation," *Geophysics* **51**, 54 (1986).
18. J. Sochacki, R. Kubichek, J. George, W. R. Fletcher, and S. Smithson, "Absorbing boundary conditions and surface waves," *Geophysics* **52**, 60 (1987).